Journal of Polymer Research (2006) 13: 507–514
DOI:10.1007/s10965-006-9073-7

Synthesis and Properties of Waterborne Polyurethane Dispersions with Ions in the Soft Segments

Li-Hong Bao[1], Yun-Jun Lan[2,*] and Shu-Fen Zhang[1]
[1]*State Key Lab of Fine Chemical, Dalian University of Technology, Dalian, Liaoning, 116012, People's Republic of China*
[2]*Zhejiang Province Key Lab of Leather Engineering, Wenzhou University, Wenzhou, Zhejiang, 325027, People's Republic of China*
*(*Author for correspondence; E-mail: blh335@21cn.com)*

Received 21 April 2006; accepted in revised form 5 July 2006; published online 13 September 2006

Key words: maleic anhydride modified castor oil, waterborne polyurethane dispersion, structure and properties

Abstract

A maleic anhydride modified castor oil (MCO) was used to prepare aqueous polyurethane dispersions (MCPUs) with ionic groups in the soft segments according to the prepolymer mixing process. The aliphatic polyether PU prepolymer was prepared with MCO and polyether glycol (Ng210) as polymeric glycol component. The prepolymer was dispersed under vigorous agitation by adding water and by chain extension with ethylene diamine. The effects of r_m (the mass ratio of MCO and Ng210) on the properties of the resultant waterborne polyurethanes (MCPUs) were studied. Structures and properties of the MCPU dispersions and their films were examined by FT-IR, particle size analyzer, DTG, DSC, WAXD, SEM and tensile tester. The MCPUs exhibit higher phase mixing with increasing of r_m.

Introduction

The waterborne polyurethane, exists as a form of aqueous dispersion, has received considerable attention in the past a few decades due to the environmental requirements and protection acts [1–3]. In addition to environmental advantage, aqueous PU dispersions can also be prepared with high solid content and high molecular weight, since the viscosity of the dispersion is generally independent of the molecular weight of the dispersed polymer particles. The film forming with it has excellent properties. The price of waterborne PU is generally low comparing to solventborne PU. So it has been used in various fields, such as textile, coating, leather and adhesives [4–6].

Polyurethanes are segmented copolymers, which consist of alternating soft and hard segment units. The soft segment is commonly a low molecular weight polyether or polyester whereas the hard segment generally consists of a diisocyanate condensed with a low molecular weight diol. It is now generally accepted that the mechanical properties of polyurethane materials are primarily due to the phase separation of soft and hard segments leading to the formation of hard segment domains, which are dispersed in the rubbery matrix [7]. There has been a wide range of work done in the synthesis and characterizations of waterborne PU [8–10]. Generally, the waterborne PU can be prepared in the ionomer and nonionomer form, notably an anionomer. One synthesis procedure is to use a chain extender containing a carboxylic acid group to produce a NCO terminated prepolymer, through phase inversion process, then chain extended with diamine [11]. Another procedure involves reacting the urethane group with a sodium hydride and subsequently reacting with 1,3-propane sultone to produce a polyurethane sulfonate [12]. However, in these previous instances the ionic groups were located in the hard segment. The effect of these ions was to increase the polarity of the hard segment and hence decrease the compatibility of the hard and soft segments [13]. Besides, the hydrophilic ionic groups can couple with the hydrophilic urethane or urea groups and augment the hydrophilicity of the hard segment. When dispersed in water, the hydrophilic segment are preferentially located on the surface of the particle, involving some water in it, which make the film formation period increase as the swelled water is difficult to evaporate [14].

In view of the disadvantages of waterborne PU with ions in the hard segment, some researchers attempted to synthesis waterborne PU with ionic groups distributed in the soft segment and studied their properties. B. K. Kim et al. [14] synthesis PU ionomer dispersions containing ionic groups in soft segment and compare it with conventional ones which contain ionic groups in hard segments. They found ionic soft segments gave a significantly lower solution viscosity, smaller particle size and greater dispersion viscosity. The delocalization of hydrophilic groups among soft segments and hard segments leading to increased soft segment-hard segment phase mixing.

Xin Wei et al. [15] synthesized a series of polyurethane ionomers with different contents of sodium sulfonate

groups in the soft segments. They found, as the ionization level increased, the compatibility of the hard and soft segments increased and the glass transition region of the soft segment became broader.

Although a certain degree of research has been performed in waterborne PU with ions in the soft segment, but they are mostly focused on the chemical raw materials. It is well know that with the development of world economics, the petrochemical resources are becoming tense, especially in these years. The use of renewable resources as substitutes for petrochemical derivatives has attracted more attention of many researchers [16–18]. Castor oil is one of the naturally and abundantly occurring, it possesses both unsaturated bond and hydroxyl functional groups [19] and has become a kind of competitive material in polyurethane industry. Castor oil can be used in polyurethane elastomers and coatings; the film made from it has excellent hydrophobicity, flexibility and cold resistance [20].

In the present work, the castor oil was esterified with maleic anhydride to get a modified castor oil (MCO) containing carboxyl groups. Then it was used as polyol to react with isophorone diisocyanate (IPDI). A series of aqueous polyurethane dispersions (MCPUs) with different content of carboxyl groups in the soft segments were synthesized by varying the mass ratio of MCO and polyether glycol (Ng210).The structures and properties of these obtained MCPU dispersions and their films were investigated by FT-IR, particle size analyzer, DTG, DSC, WAXD, SEM and tensile tester.

Experimental

Materials

Castor oil (CO) and polyether glycol (Ng210: tetrahydrofuran-oxide propylene copolymer glycol, M_n = 1,000 g mol^{-1}, hydroxyl value = 102 mg KOH/g) obtained from Shanghai Chemical Co., China were dried for 48 h under a vacuum prior to use. Maleic anhydride was obtained from Shanghai Lingfeng Chemical Co., China. Isophorone diisocyanate (IPDI) was obtained from Bayer AG. Dimethylol propionic acid (DMPA), 1,4-butanediol (BD), *N*-methyl-2-pyrrolidone (NMP), triethylamine (TEA) were obtained from Shanghai Aisi Chemical Co., China. Dibutyltin dilaurate (DBTL) and ethylenediamine were obtained from Shanghai Chemical Co.

Preparation of maleic anhydride modified castor oil (MCO)

Synthesis reaction of modified castor oil (MCO) was conducted in a round bottom, four-necked flask. A weighed amount of castor oil was placed in the reactor and heated to 40 °C with a mild agitation. While keeping the temperature at 40 °C, calculated maleic anhydride dissolved in butanone were added to the reactor dropwise. Then the system was heated to 70 °C and reacted for 2 h, after that, the system was heated to 75 °C and continue reacted for 4–5 h. A modified castor oil (MCO) with a hydroxyl value of 112 mg KOH/g and an acid number of 42 mg KOH/g was obtained after evaporating butanone.

Preparation of aqueous polyurethane dispersions (MCPUs)

Polyaddition reaction was conducted in a round bottom, four-necked flask. Basic recipes for the synthesis of MCPUs were presented in Table 1. MCO and Ng210 were charged into the reactor and heated to 120 °C to dehydrate under vacuum for 2 h. Then, the system was cooled to 60 °C, IPDI and DBTL were added into the reactor and reacted for about 1 h. After that, BD and DMPA dissolved in NMP were charged into the mixture and the system was heated to 70 °C for about 2 h to afford NCO-terminated prepolymer. The change of the NCO content during the reaction was determined using a standard dibutylamine back titration method. When the NCO content reached the theoretical value, the reaction mixture was cooled to 50 °C and neutralized by adding TEA. Then the doubly distilled (DD) water was slowly charged into the obtained anionomer and the polymer chain was extended by reacting with ethylene diamine.

Characterization

The average particle diameters and particle size distributions of MCPU dispersions were determined by a BT-9300S particle size analyzer.

^{1}H n.m.r. spectra were recorded at room temperature using a Avance-300 spectrometer. Concentration of MCO or CO is 5% (w/v) in $CDCl_3$.

FT-IR spectra were recorded with Bruker EQUINOX 55 spectrometer.

The MCPU films were prepared by casting the aqueous dispersions on leveled surfaces and allowing them to dry at room temperature for seven days, and then at 60 °C, for 12 h.

Thermogravimetric experiments were performed on a SDTQ 600 analyzer. Film samples ranging from 5 to 7 mg and heated from 30 to 500 °C under N_2 atmosphere at a heating rate of 10 °C/mm.

Table 1. Batch charging scheme for the preparation of MCPUs.

Ingredients	Charge (g) MCPU01	MCPU12	MCPU11	MCPU21	MCPU10
MCO[a]	–	6.66	10.0	13.33	20.0
Ng210	20.0	13.33	10.0	6.67	–
IPDI[b]	17.76	17.76	17.76	17.76	17.76
DMPA[c]	2.70	2.06	1.75	1.43	0.79
BD	1.52	1.957	2.16	2.38	2.80
TEA[d]	2.03	2.03	2.03	2.03	2.03
DD water	181.56	180.88	180.0	179.84	179.0
EDA	1.37	1.37	1.37	1.37	1.37

[a]The r_m (the mass ratio of MCO and Ng210) of MCPU10, MCPU21, MCPU11, MCPU12 and MCPU01 is 1:0, 2:1, 1:1, 1:2, 0:1 respectively.
[b]The ratio of NCO/OH is fixed to 1.4.
[c]The content of –COOH is 2.0% on the basis of the solid content of the MCPU aqueous dispersions.
[d]The neutralization degree of –COOH in MCPUs is 100%.

Differential scanning calorimetric measurements of MCPU films were carried out on a NETZSCH DSC 204 thermal analyzer. The heating rate was 10 °C/min between −100 and 30 °C under N_2 atmosphere.

Morphologies of MCPU films were examined with a scanning electron microscope JSM-6700. The specimens were mounted on an aluminum stub and sputter-coated with a thin layer of gold to avoid electrostatic charging during examination.

Wide-angle X-ray diffraction(WAXD) patterns of the MCPU films were recorded on D/max-1200 X-ray diffractometer with Cu Kα radiation($\lambda = 1.5405 \times 10^{-10}$ m), and the samples were examined with 2θ ranging from 5 to 50° at a scanning rate of 5° min^{-1}.

The mechanical properties of the MCPU films were evaluated by tensile testing. Dumbbell-shaped specimens were prepared by stamping a sheet of the MCPU films with a standard die in accordance with ASTM D638-Type IV. The tensile test was performed at a cross-head speed of 100 mm/min. Tensile strength, elongation at break; elastic modulus and hardness of each specimen were averaged from five tests.

Each of the MCPU film was cut into 30 mm × 30 mm sample and stored in different solvents for 24 h. Excess of the solvent on the film surface was removed with a filter paper. Then, the film was weighed and the absorptivity of solvent (SA%) was calculated using the following equation:

$$\mathrm{SA}\% = \frac{W_2 - W_1}{W_1} \times 100$$

Where W_1, is the mass of the dry sample and W_2 the mass of the sample after absorption of the solvent.

Results and discussion

Average particle diameters and particle size distributions of MCPU dispersions

Figures 1 and 2 show the particle size distributions and the average particle diameters of MCPU dispersions. In PU dispersions, the average particle size is governed mainly by the hydrophilicity of the PU [21, 22]. However, the carboxyl groups in the present systems are fixed to a same content, so the particle distributions and the average particle diameters are mainly affected by the mass ration of MCO and Ng210 (r_m). It was found that the least particle diameter is 29.5 nm and the particle size distribution is narrowest when r_m is 1:2. A possible explanation for this is that, in MCPU01, the hydrophilic carboxyl groups are all located in the hard segments, the polymer chains are well arranged and the soft segments tend to assemble to form larger particles. When MCO was incorporated into MCPU, the soft segments were consisted of MCO and polyether, the MCO molecules are ramified and contain carboxyl groups, which make the polymer tend to more compatible with water to form smaller dispersed particles. But the dispersion became broader and the average particle diameter shifted to higher value from 29.5 nm to 105.8 nm with increasing of r_m from 1:2 to 1:0. As r_m increases, the content of carboxyl in the soft segments increases, since the charge of DMPA decreases, the random structure of MCO can inhibit the segments to form ordered domain, resulting in increasing of phase mixing of soft and hard segments. Moreover, the hydrogen-bond increases with r_m increases, the intermolecular interaction can cause the polymer chains aggregate to form larger dispersion particles. In addition, the irregularity of such polymer chains and aggregation states will cause a broader particle size distribution.

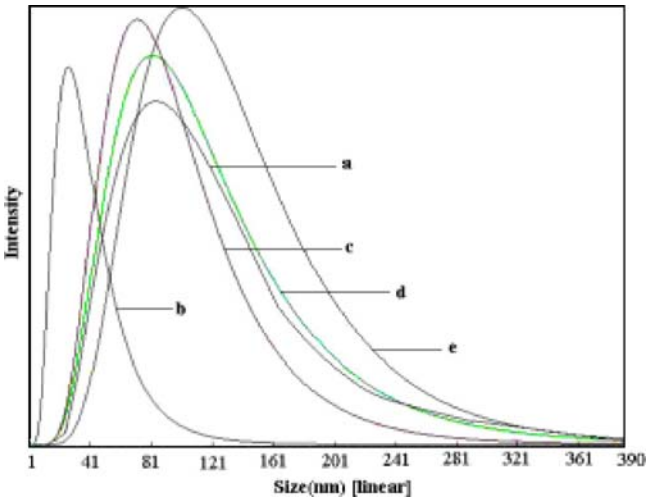

Figure 1. Particle size distributions of MCPU dispersions. (a) MCPU01, (b) MCPU12, (c) MCPU11, (d) MCPU21, (e) MCPU10.

(a) MCPU01; (b) MCPU12; (b) MCPU11; (c) MCPU21; (d) MCPU10

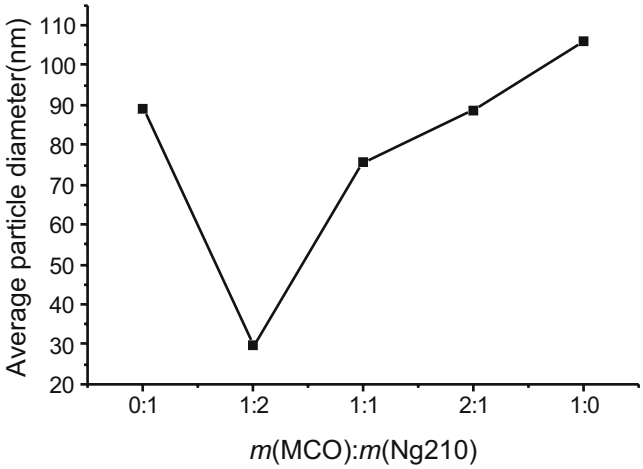

Figure 2. Average particle diameters of MCPU dispersions.

^{1}H-NMR spectra of CO and MCO

Figure 3 is the ^{1}H-NMR spectrum of CO and MCO. The esterification of CO was confirmed by ^{1}H-NMR, acid number and hydroxyl value determination. The ^{1}H-NMR spectrum of MCO showed two peaks at 6.48 (a) and 6.35 (b) ppm due to the anhydride group adjacent to the hydroxyl group; these two peaks were not observed before

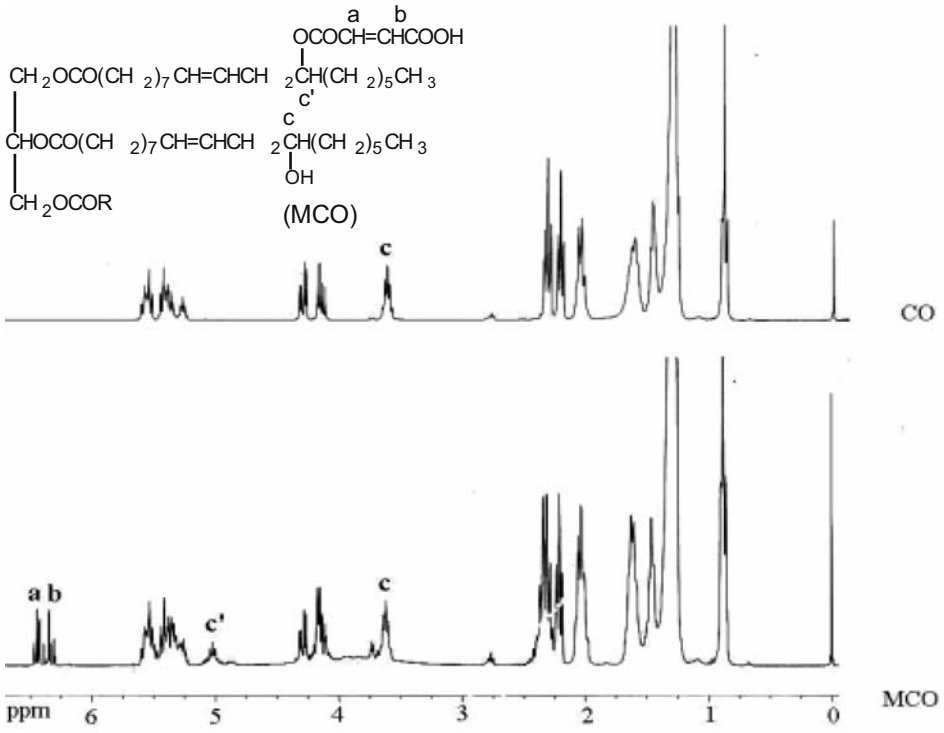

Figure 3. ^{1}H-NMR spectra of CO and MCO.

esterification. Moreover, part of absorption peaks of ricinoleyl's methine proton c (at α-C of the hydroxyl group of CO) at 3.6 ppm shifted down-field in the δ 4.9–5 ppm region becoming c′ (carboxylate). From the acid number and hydroxyl value determination of MCO, it is confirmed that part of the hydroxyl groups of CO reacted with maleic anhydride.

FT-IR spectroscopy

The IR absorption spectra of CO, MCO and MCPU11 dispersion are shown in Figure 4. Strong absorption bands appear separately at 3,470–3,500 cm^{-1} (νOH), 2,932 cm^{-1} and 2,860 cm^{-1} (νC–H, CH_3– or –CH_2–). After modification, the absorption peak of methyl and methylene of CO change little, but the absorption peak area of –OH decreases

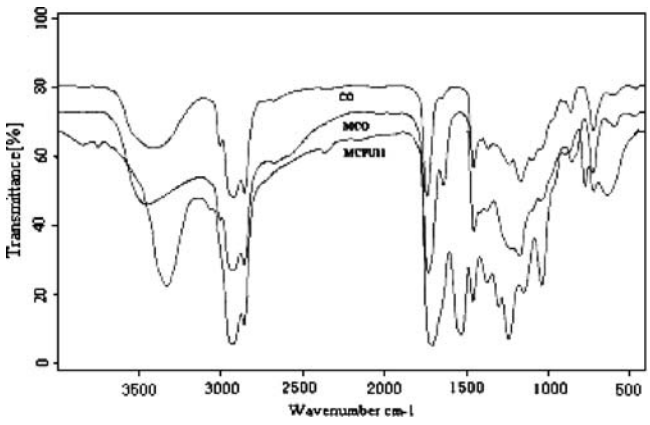

Figure 4. IR spectra of CO, MCO and MCPU11.

obviously and becomes broader, a stretching vibration for conjugate carboxylic acid appears at 1,690–1,710 cm^{-1}. This implies that an esterification happened between maleic anhydride and castor oil and a few carboxylic acid groups were introduced into CO. In MCPU11 absorption spectrum, no –NCO stretching peak at 2,270 cm^{-1} has been observed.

Figure 5 shows the IR spectra of MCPU dispersions. In order to identify the structure differences of these samples, the three main regions absorption were also presented once again.

1. 3,200–3,550 cm^{-1} N–H stretching, a broad absorption band was composed of two peaks. The higher frequency at about 3,444 cm^{-1} was due to free –NH stretching while the peak at around 3,350 cm^{-1} was due to H-bonded –NH stretching.
2. 1,680–1,750 cm^{-1} C = O stretching, the carbonyl stretching absorption band was also observed to be composed of two peaks, 1,734 cm^{-1} was assigned to free carbonyl stretching and 1,702 cm^{-1} was attributed to H-bonded carbonyl stretching.
3. 1,000–1,150 cm^{-1} C–O–C stretching.

FT-IR spectra have demonstrated H-bonding in PU [23, 24]. The N–H group could form hard-hard segment H-bonding with the carbonyl oxygen and hard–soft segment H-bonding with the ether oxygen and carbonyl oxygen in the present system. In general, the strength of hard–hard segment H-bonding is stronger than that of hard–soft segment H-bonding [25]. Whereas, the fraction of hard–hard segment H-bonding was usually used as a measure of the extent of phase separation, and hard–soft segment H-bonding represent the extent of phase mixing between hard and soft segments [26–30]. Figure 5 shows that, with r_m increases,

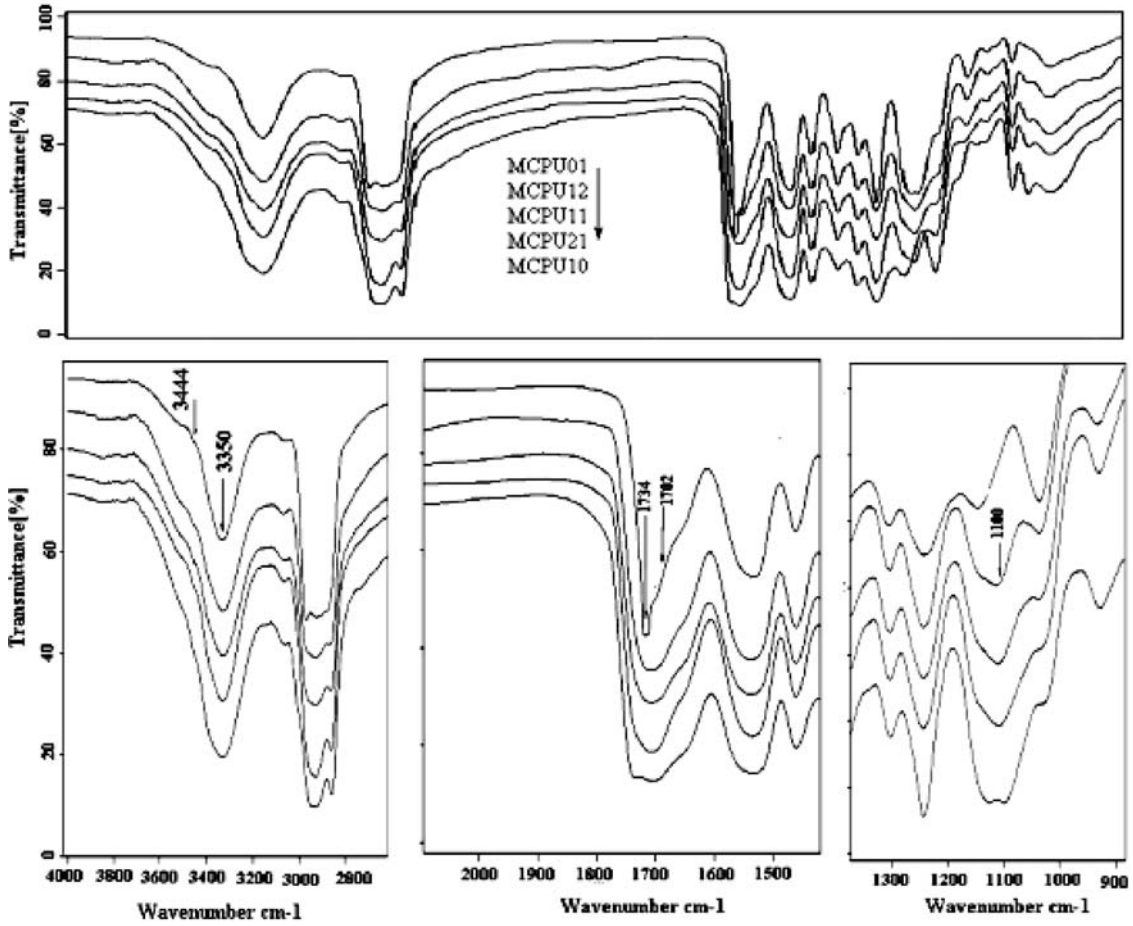

Figure 5. IR spectra of MCPU dispersions with various r_m.

more H-bonded –NH absorption was observed. This is presumably due to the carbonyl group in MCO is more polarized than ether group in Ng210, thus exhibiting a stronger hydrogen-bonded ability. The free and H-bonded C = O stretching increase with r_m increases was also shown in Figure 5. This is mainly attributed to more carbonyl groups were introduced by more MCO; they can H-bonded with –NH. So these IR spectra indicate that phase mixing increases with increasing of r_m. In addition, the absorption of C–O–C at 1,100 cm−1 decreases with Ng210 decreases.

DSC

Figure 6 shows the TG-DSC thermograms of five MCPU films. Table 2 shows the DSC scan results of these samples. A soft-segment Tg_1 of −56 °C and a hard-segment Tg_2 of 60.3 °C for MCPU01 were observed, and the transition at 60.3 °C is attributed to the disruption of

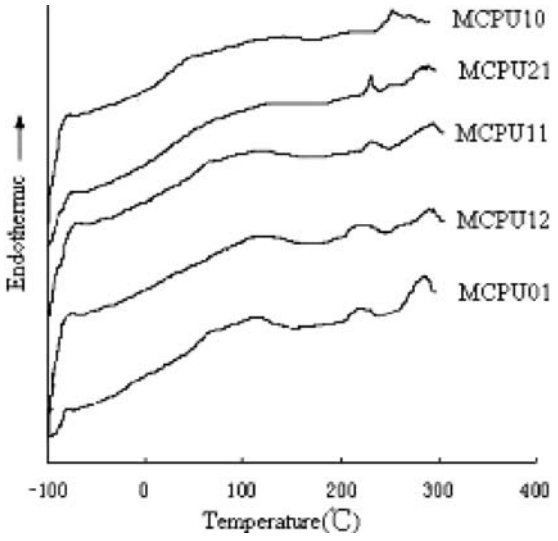

Figure 6. TG-DSC curves for MCPU films with various r_m.

Table 2. DSC scan results for MCPU films with various r_m.

Sample	Tg_1 (°C)[a]	Tg_2 (°C)[a]	Ta_1 (°C)[b]	$_{\Delta}Ha_1$ (J/g)[c]	Ta_2 (°C)[b]	$_{\Delta}Ha_2$ (J/g)[c]
MCPU01	−56	60.3	125	5.24	221	6.79
MCPU12	−51	56.7	140	3.26	222	4.37
MCPU11	−47	52.4	141	1.42	224	2.14
MCPU21	–	37.2	148	0.36	230	1.83
MCPU10	–	23.6	–	–	–	–

[a]Glass transition temperature
[b]Temperature of endotherm peak
[c]Heat capacity of endotherm peak

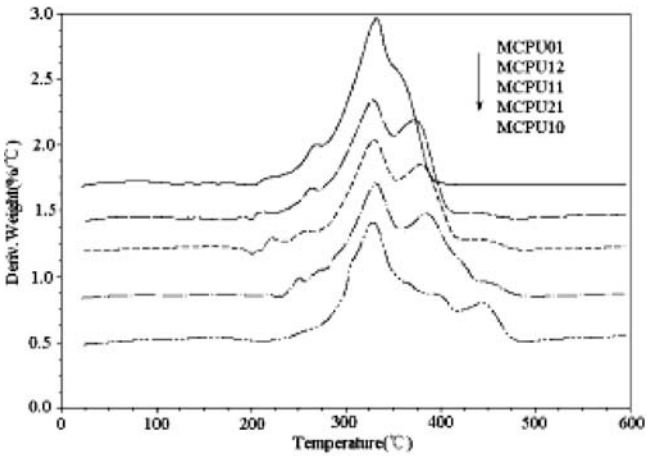

Figure 7. DTG curves of MCPU films with various r_m.

hard domains with limited short range order [31]. Moreover, two endothermic disintegration at about 125 °C(I) and 221 °C (II) appear. The endothermic disintegration I represents disordering of hard segments with relatively long-range order, whereas the endotherm II is melting of microcrystalline ordering of hard-segment domains [32]. With r_m increases from 0:1 to 1:1, the Tg_1 for soft segments increases from −56 °C to −47 °C, and no Tg_1 was observed for MCPU21 and MCPU10, while the Tg_2 for hard segments decreases from 60.3 °C to 23.6 °C, the heat capacity at I and II decrease. These results indicate that the regular arranged hard segments decrease and phase compatibility between hard and soft segments improve. This might be due to more carboxyl groups were incorporated into soft segments with increasing of MCO, the polarity difference between soft and hard segments decreased and the distribution of hydrogen bond in polymer chains altered, which has been proved in IR study. In addition, the branched MCO chains can inhibit the arrangement of segments, resulting in higher phase mixing. The MCPU10 made from MCO as soft segment only has one wide glass transition at about 23.6 °C.

Table 3. TG data obtained for the MCPU samples.

Sample	$T_{10\%}$ (°C)[a]	$T_{50\%}$ (°C)[b]	$T_{90\%}$ (°C)[c]	T_{max1} (°C)[d]	T_{max2} (°C)[e]	T_{max3} (°C)[f]	Residue at 500 °C (%)[g]
MCPU01	259.6	327.1	367.3	323	358	–	0.47
MCPU12	261.7	336.5	396.8	328.6	373.3	442.5	3.4
MCPU11	260.6	344.5	474.2	330.5	380.6	450	4.9
MCPU21	275.4	347.1	427.2	332.3	386	456	4
MCPU10	263	341	444.5	329	398	446	3.9

[a]Temperature for 10% of weight loss
[b]Temperature for 50% of weight loss
[c]Temperature for 90% of weight loss
[d]Temperature at maximum rate of weight loss of first step
[e]Temperature at maximum rate of weight loss of second step
[f]Temperature at maximum rate of weight loss of third step
[g]Residual percentage of weight at 500 °C

DTG

Figure 7 presents the differential weight loss (DTG) curves of MCPU films with different r_m. These curves show a weight loss less than 5% at 200–240 °C, that is probably associated with the release of trapped solvent and the degradation of oxidative products of MCO contained double bond [33]. Then a big weight loss occur at about 250 °C related to the degradation of hard segments [34].

The temperature of maximum rate of weight loss T_{max1} (°C; Table 3) is lower for the sample with the highest content of Ng210 and increases from 323 °C to 332.3 °C as increasing of r_m from 0:1 to 2:1. The next weight loss stage probably associated with soft segment degradation is shifted to higher temperature in the maximum rate of weight loss T_{max2} (°C) from 358 °C to 398 °C with r_m increases from 0:1 to 1:0. The third weight loss stage is above 400 °C. These curves show more complex degradation behaviors with r_m increases. This indicates the degradation reduces with increasing of r_m. The fact might be attributed to the branched MCO can produce strong intermolecular interaction, the carboxyl located in soft segment can form higher cohesive energy and the polyurethane contained MCO has more hydrogen bond as indicated by the IR results.

WAXD

X-ray diffraction patterns for these MCPU films are shown in Figure 8. The broad scattering halos between 5° and 50° of 2θ are presented in all samples. This indicates that all samples are amorphous at room temperature.

Morphology of the MCPU films

The SEM photographs of the cross section of MCPU films with various r_m are shown in Figure 9. The hard-segment

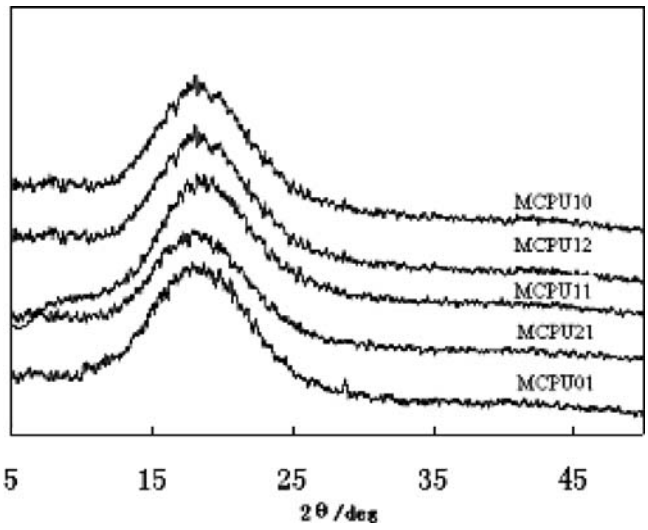

Figure 8. WAXD spectra for MCPU films with various r_m.

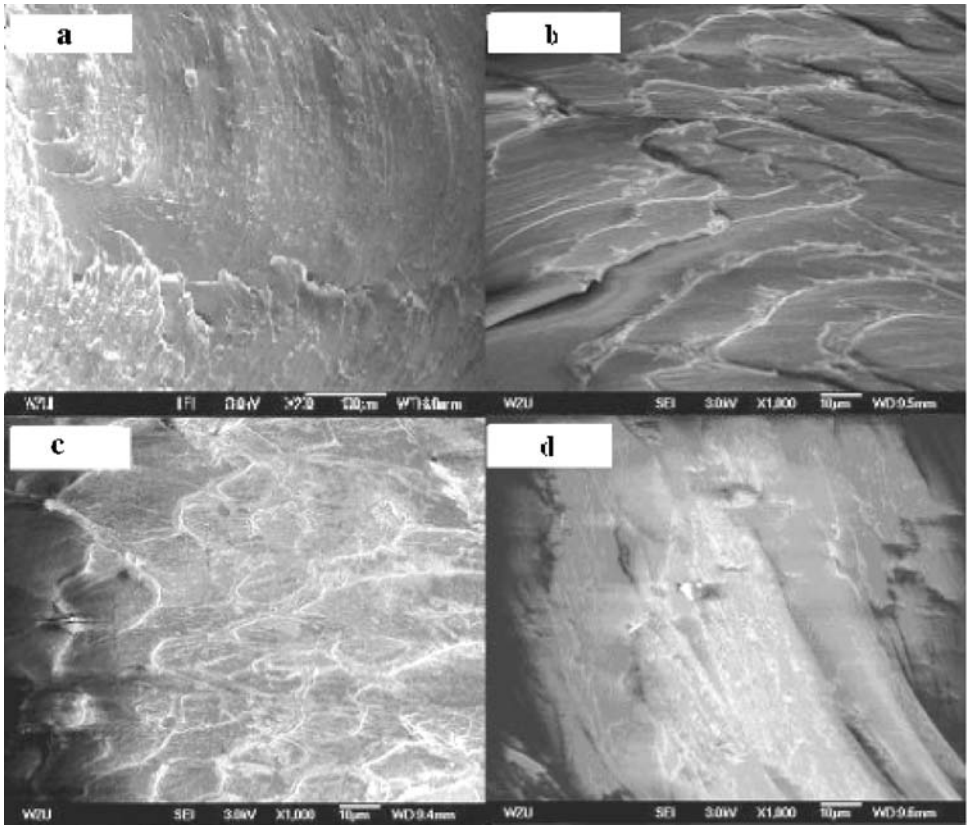

Figure 9. The SEM photographs of the cross section for MCPU films: (a) MCPU12 × 200; (b) MCPU11 × 1000; (c) MCPU21 × 1000; (d) MCPU10 × 1000.

domains are very clear in the cross section of the films with lower r_m. It can be observed that the hard-segment domains distribute in the soft matrix in MCPU12 at the magnification of 200. The phase separation decreases with increasing of r_m and the hard-segment domains become inconspicuous. It hardly can observe the hard domain in MCPU10. These results imply that the phase mixing increases with r_m increases, it has also been identified by DSC results.

Mechanical properties and solvent absorptability of MCPU films

The mechanical properties of polyurethane were generally accredited to the result of a pseudo-crosslinking effect resulting from the hard-segment aggregation distribute in the soft matrix [35].The results of physic-mechanical measurements of MCPU films are presented in Table 4, It is evidenced that an increase of r_m leads to a higher tensile strength, modulus and hardness except for MCPU10, which may be explained by increasing of hydrogen bond (NH... O = C < =), resulting in a higher physical crosslinkings through the intermolecular interaction. A difference in the domain morphology would also likely lead to a significant difference in the ultimate tensile properties. As Smith [36] and Cooper [37] speculated, interconnected or interlocked domain morphology would exhibit higher ultimate tensile strength than separated domain morphology. While the decreasing of elongation at breaking from 825.3% to 121.5% with the increasing of r_m from 0:1 to 1:0 can be attributed to the physical crosslinking and branched structure of MCO, which could decrease the flexibility of polymer chains. The strange behaviors of the mechanical properties of MCPU10 are presumably due to the excessive hard segments were solved in soft matrix; few ordered hard domains were formed.

Table 4. Mechanical properties of MCPU films.

Sample	Tensile strength (MPa)	Elongation at break (%)	Hardness (shore A)	Elastic modulus (MPa)
MCPU01	8.06	825.3	25	35.6
MCPU12	12.3	557.6	32	52.7
MCPU11	22.31	289.5	45	78.6
MCPU21	24.52	187.2	47	82.3
MCPU10	13.46	121.5	38	62.4

Table 5. Solvent absorptivity of MCPU films with various r_m.

Sample	SA(%) Water	SA(%) toluene
MCPU01	51	156.89
MCPU12	26.42	104.82
MCPU11	18.6	98.45
MCPU21	14.35	93.97
MCPU10	11.22	75.56

The solvent absorptivity of MCPU films were shown in Table 5. With the increasing of r_m, the swelling in water and toluene was decreased. The crosslinking and hydrophobic aliphatic chains in MCO and high dispersed carboxyl distribution in higher r_m improve the water resistance of polymer. The higher crosslinking degree produces better toluene resistance.

Conclusions

In this study, aqueous polyurethane dispersions (MCPU) with ions in the soft segments were prepared from maleic anhydride modified castor oil (MCO) and Ng210 with various mass ratio according to the prepolymer mixing process. The dispersion's particle diameter is least 29.5 nm and the particle size distribution is narrowest when r_m (the mass ratio of MCO and Ng210) is 1:2, which is attributed to the ramified structure of MCO and the more distributed carboxyl groups. IR spectra of CO, MCO and MCPU films identified that conjugate carboxylic groups and the hydrogen bonding increase with increasing of MCO components in MCPU. TG-DSC curves showed that Tg_1 for soft-segment increased, Tg_2 for hard-segment decreased, and the heat capacity for the endothermic of long-range ordered hard segment and microcrystalline ordering of hard-segment domains decreased as r_m increases. These results implied that the phase mixing increased with increasing of r_m. This is also identified by SEM photo further. The DTG study showed that heat decomposition behaviors of MCPU films became complex and shifted to higher temperature as r_m increases, this is due to the strong intermolecular interaction resulting from the branched MCO and higher content of hydrogen bonding, the carboxyl groups located in soft segment can form higher cohesive energy. The MCPU films' tensile strength, modulus and hardness increased as r_m increases except for MCPU10 is may be explained by the higher hydrogen bond (NH...O = C < =), and the increasing of the intermolecular interaction resulting from physical crosslinking. The poorer mechanical properties of MCPU10 are presumably due to the excessive phase mixing. With the increasing of r_m, the swelling in water and toluene was decreased is mainly ascribed to the higher physical crosslinking degree of the polymer.

Acknowledgments

The authors thank Mr. Luo Weiping, Yin Dehai and Professor Li Linsheng for their constant encouragement and suggestions throughout the work.

References

1. Y. K. Jhon, I. W. Cheong and J. H. Kim, *Colloids Surf., A Physicochem. Eng. Asp.*, **179**, 71 (2001).
2. L. K. Saw, B. W. Brooks, K. J. Carpenter, et al, *J. Colloid Interface Sci.*, **257**, 163 (2003).
3. Y. S. Kwak, S. W. Park and H. D. Kim, *Colloid Polym. Sci.*, **281**, 957 (2003).
4. Harro Traubel, Karl Pisaric and Michael Traubel, US 2001/0 031 363 A1, 10-18-2001.
5. Wilhelm Thoma, Klaus Nachtkamp, Walter Schroer and Rolf Langel, US 4 543 144, 9-24-1985.
6. Wolfgang Henning, Walter Meckel and Peter Fuhrmann, US 4 857 565, 8-15-1989.
7. N. S. Scheider, C. S. Paik Sung, R. W. Matton and J. L. Illinger, *Macromolecules*, **8**, 62 (1975).
8. A. K.Nanda, D. A.Wicks, S. A. Madbouly, et al, *J. Appl. Polym. Sci.*, **98**, 2514 (2005).
9. S. S. Yoon and S. C. Kim, *J. Appl. Polym. Sci.*, **95**, 1062 (2005).
10. T. C.Wen, Y. J. Wang, T. T. Cheng, and Ch. H. Yang, *Polymer*, **40**, 3979 (1999).
11. M. C. Delpech and F. M. B. Coutinho, *Polym. Test.*, **19**, 939 (2000).
12. H. Sh. Xu, and Ch. Zh. Yang, *J. Polym. Sci., B, Polym. Phys.,* **33**, 745 (1995).
13. Ch. Zh. Yang, T. G. Grasel, J. L. Bell, et al, *J. Polym. Sci., B,* Polym. Phys., **29**, 581 (1991).
14. B. K. Kim, J. S. Yang, S. M. Yoo, et al, *Colloid Polym. Sci.,* **281**, 461 (2003).
15. W. Xin and X. H. Yu, *J. Polym. Sci., B, Polym. Phys.*, **35**, 225 (1997).
16. H. D. Rozman, Y. S. Yeo, G. S. Tay, et al, *Polym. Test.,* **22**, 617 (2003).
17. S. D. Desia, A. L. Emanuel and V. K. Sinha, *J. Polym. Res.*, **10**, 141 (2003).
18. J. Huang and L. Zhang, *Polymer*, **43**, 2287 (2002).
19. M. Begum and Siddaramaiah, *J. Mater. Sci.*, **39**, 4615 (2004).
20. S. Bai, D. V. Khakhar and V. M. Nadkarni, *Polymer*, **38**, 4319 (1997).
21. C. K. Kim, B. K. Kim and H. M. Jeong, *Colloid Polym. Sci.*, **269**, 895 (1991).
22. T. K. Kim, B. K. Kim, *Colloid Polym. Sci.*, **269**, 889 (1991).
23. S. K. Pollack, D. Y. Shen, S. L. Hsu, et al, *Macromolecules*, **22**, 551 (1989).
24. C. S. P. Sung and N. S. Schneider, *Macromolecules*, **l8**, 68 (1975).
25. Z. Petrovic, *J. Polym. Sci., B, Polym. Phys.*, **33**, 745 (1995).
26. D. J. Martin, G. F. Meijs, G. M. Renwick, et al, *J. Appl. Polym. Sci.*, **62**, 1377 (1996).
27. D. J. Martin, G. F. Meijs, G. M. Renwick, et al, *J. Appl. Polym. Sci.*, **60**, 557 (1996).
28. M. S. Yen and S. C. Kuo, *J. Appl. Polym. Sci.*, **61**, 1639 (1996).
29. L. S Teo, C. Y. Chen and J. F. Kuo, *Macromolecules*, **30**, 1793 (1997).
30. J. D. Van Heumen and J. R. Stevens, *Macromolecules*, **28**, 4268 (1995).
31. R. W. Seymour and S. L. Cooper, *Macromolecules*, **6**, 48 (1973).
32. C. B. Wang and S. L. Cooper, *Macromolecules*, **16**, 775 (1983).
33. S. Sarkar and B. Adhikari, *Polym. Degrad. Stab.*, **73**, 169 (2001).
34. T. L. Wang and T. H. Hsieh, *Polym. Degra. Stab.*, **55**, 95 (1997).
35. L. L. Harrell Jr, *Macromolecules*, **l2**, 607 (1969).
36. T. L. Smith, *Polym. Eng. Sci.*, **17**, 129 (1977).
37. R. W. Seymour and S. L. Cooper, *Rubber Chem. Technol.*, **47**, 19 (1974).